Comparative study on various morphologies of WS_2 for electrochemical hydrogen evolution reaction

Ha Huu Do*, Duc Anh Dinh, The Duy Nguyen, Truc Phuong Nguyen Tran, Manh Dang Le

VKTech Research Center, NTT Hi-Tech Institute, Nguyen Tat Thanh University
*dhha@ntt.edu.vn

Abstract

Nowadays, the advancement of cost-effective and efficient electrocatalysts holds significant importance in facilitating the progress of high-performance electrochemical hydrogen evolution reaction (HER). Tungsten disulfides (WS_2) are well recognized as highly promising electrocatalysts for HER due to their exceptional catalytic performance, outstanding stability, and comparatively affordable price. In this study, we used ammonium metatungstate hydrate and thioacetamide as precursors to fabricate WS_2 nanoflowers (NFs) by hydrothermal method, whereas WS_2-flakes were prepared from ammonium tetrathiotungstate through the thermolysis technique. These structures were evaluated for HER electrocatalytic activity in acidic media. The results revealed that WS_2-NFs exhibit higher catalytic activity than WS_2-flakes, with an overpotential of 325 mV to obtain a current density of 10 mA cm^{-2} and a Tafel slope of 92.3 mV dec^{-1}. This performance was attributed to the larger electrochemically active surface area of WS_2-NFs compared to WS_2-flakes materials. The results of this study could bring the basis for further studies on the synthesis of WS_2-based catalytic materials for HER.

Received 02/11/2023
Accepted 29/11/2023
Published 29/12/2023

Keywords
WS_2, electrocatalysts, hydrogen evolution reaction, nanoflowers, morphology

1 Introduction

The utilization of fossil fuels for energy generation has resulted in the emission of a substantial quantity of carbon dioxide (CO_2), leading to the phenomenon of climate change and environmental contamination. Hence, the pursuit of environmentally friendly and sustainable fuel alternatives is imperative on a global scale. Hydrogen is often regarded as a highly promising fuel source for future energy demands. Hydrogen exhibits superior energy density in comparison to conventional sources such as coal, methane, and gasoline [1-3]. Furthermore, the combustion of hydrogen yields water as a by-product, rendering it highly ecologically sustainable. At present, hydrogen can be generated by various methodologies, including coal gasification, methane gas reforming, and water electrolysis [4-8]. Nevertheless, the initial two techniques release CO_2 during the hydrogen production process, exerting a detrimental impact on the environment. The electrochemical hydrogen evolution reaction (HER) process is often regarded as the most promising approach for hydrogen production because of its ability to meet the criteria of environmentally friendliness, efficiency, and sustainability. To date, the most optimal performance in the field of HER has been achieved by employing precious metal catalysts, namely platinum (Pt), palladium (Pd), and rhodium (Rh). [9-12]. However, the scarcity and high cost of these materials have prompted extensive research efforts, both experimental and theoretical, aimed at discovering alternative materials that are more affordable yet possess superior performance characteristics. For instance, transition metal sulfides,

https://doi.org/10.55401/9f312g30

selenides, and oxides have been investigated for HER. [13-15]. Among these electrocatalysts, transition metals sulfides are promising materials for hydrogen production by electrochemical method. It is worth noting that WS_2-based materials have been extensively examined as prospective alternatives to costly metal-based catalysts for the process of HER owing to their exceptional stability and superior performance. Several strategies have been suggested in previous literature to enhance the catalytic performance of WS_2, including doping, utilization of carbon-based support materials, and manipulation of the phase structure. For example, Sun et al. introduced nitrogen doping onto WS_2 nanosheets. The outcomes of their research demonstrated favorable results, as they achieved an overpotential for water splitting that was below 100 mV [16]. Lei et al. successfully synthesized WS_2/C composites that exhibit exceptional catalytic properties. These enhanced HER activities can be attributed to the higher conductivity and active surface area associated with the incorporation of carbon in the composite material [17]. Also, Lukowski and colleagues created phase 1T WS_2 from phase 2H-WS_2 with very high efficiency for HER [18]. Although WS_2-based catalysts for HER have been published, studies on the relationship between the morphological structures and catalytic activities of this material have not been systematically studied. In this study, various morphologies, including WS_2 nanoflowers (NFs) and WS_2- flakes forms were fabricated and evaluated for their catalytic activity for hydrogen production.

2 Materials and methods

2.1 Materials and chemicals

Ammonium metatungstate hydrate (≥85 % WO_3 basis), thioacetamide (98 %), ammonium tetrathiotungstate (99.9 %), Nafion (5 %), và sulfuric acid (98 %) were provided by Sigma Aldrich.

2.2 Preparation of WS_2 with various morphologies

Preparation of WS_2-NFs. The aforementioned structure was fabricated via the hydrothermal technique. Compared to Hasani's study, WS_2-NFs were synthesized at a lower temperature and shorter reaction time [19-21]. Initially, a quantity of 8 g of thioacetamide was agitated within a glass vial that contained 40 mL of deionized water for 60 minutes. Subsequently, 8 g of ammonium metatungstate hydrate was introduced into the mixture, followed by continuous stirring for 60 minutes. The mixture was placed into a Teflon autoclave reactor and subjected to a thermal treatment at a temperature of 180 °C for a period of 20 hours. After the reaction was finished, the reactor was subjected to a cooling process at 25 °C. Next, the solid was carefully separated and subsequently rinsed using centrifugation, repeating the process three times using deionized water. Finally, the WS_2 catalyst underwent a drying process at 100 °C in a vacuum environment for 12 hours, resulting in the production of the final powdered product.

Preparation of WS_2-flakes. This structure is produced by pyrolysis according to the following procedure [22]. A total of 8 g of ammonium tetrathiotungstate were placed in a ceramic crucible before being transferred to an inert gas furnace and heated to 900 °C for 2 hours. Following the end of the reaction, the furnace was then cooled down to ambient temperature. The obtained solid product was then isolated and subjected to a thorough washing process using centrifugation. This washing procedure involved three times of rinsing with deionized water. Finally, the WS_2 material was dried at 100 °C under vacuum for 12 hours. The formation of WS_2 was presented in the following:

$$(NH_4)_2WS_4 \rightarrow WS_2 + 2NH_3 + H_2S + S \qquad (1)$$

2.3 Material characterization

Scanning electron microscopy (SEM) was conducted to identify various morphologies of WS_2 materials on Zeiss Sigma 300 equipment. The crystal structure of WS_2 materials was analyzed by the X-ray diffraction (XRD) method on equipment of the Bruker D8-Advance.

2.4 Catalytic activities evaluation

The electrocatalytic activities of the WS_2-NFs and WS_2-flakes were evaluated on a conventional electrochemical system in 0.5 M H_2SO_4 acidic medium. All electrochemical measurements were conducted on a potentiostat (Ivium 5612, Netherlands). The reference electrode used in the experiment was the saturated calomel electrode (SCE). The carbon rod was employed as the counter electrode. The fabrication of the working electrode is carried out under the following technique. The catalyst suspension was formed by combining 10 mg of WS_2 material with 5 mL of deionized water and 0.5 mL of Nafion, then the mixture was sonicated for 60 minutes at 25 °C to obtain the catalytic ink, after which 1 mL of this ink was coated to the surface of the glassy carbon electrode and parched at 90 °C for 30 minutes to create a working electrode. During the electrochemical experiments, linear sweep voltammetry was recorded at a scan rate of 2 mV s^{-1}. All obtained potentials were converted by the formula, $E_{RHE} = E_0 + E_{SCE} + 0.059$ pH. Electrochemical impedance spectroscopy (EIS) was implemented in a frequency range from 0.1 to 100,000 Hz. The stability of WS_2 was evaluated by chronoamperometry during 10 hours and cyclic voltammetry (CV) with 2000 cycles.

3 Results and discussions

The crystal structure of the WS_2 material was examined by XRD method as shown in Figure 1. WS_2-flakes catalysts have diffraction peaks at 14.3°, 32.7°, 39.5°, and 58.4° are designated the (002), (100), (103), and (110) crystal facets of the 2H-WS_2 hexagonal phase structure [19, 23, 24]. Moreover, the high-intensity peak of (002) revealed that WS_2-flakes were stacked together with a highly ordered packing, whereas WS_2-NFs displayed low-intensity peaks with the peak of the (002) crystal plane changed to diffraction angle position $2\theta \sim 13.8°$. This result revealed that the number of stacks of (002) crystal planes was decreased for the WS_2-NFs sample. Besides, no strange peaks indicate the high purity of the generated WS_2 catalysts. Figure 2 illustrated the SEM images of the different morphologies of the WS_2 catalyst. Figure 2a displays the nanoflower morphology of the WS_2 material with a smaller size than the WS_2-flakes catalyst (Figure 2b). This result implies that WS_2-NFs give a higher active surface area than WS_2-flakes.

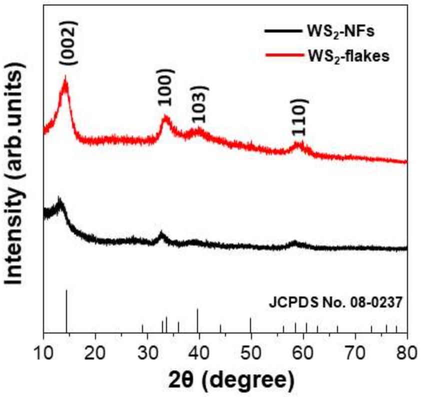

Figure 1 XRD patterns of WS_2-NFs and WS_2-flakes

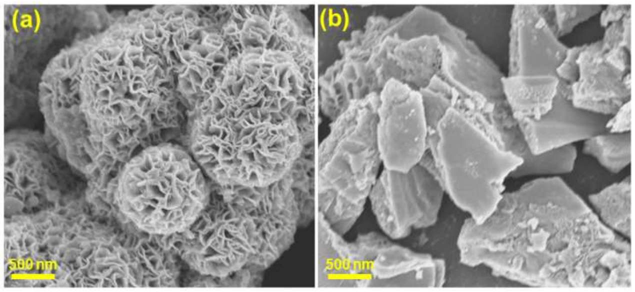

Figure 2 SEM of (a) WS_2-NFs and (b) WS_2-flakes

The HER electrocatalytic activity of the WS_2 structural morphologies was evaluated in an acidic medium. The polarization curves are shown in Figure 3a. This graph shows that the WS_2-NFs have a lower voltage requirement than the WS_2-flakes at 10 mA cm^{-2}. In particular, overpotential values are 325 mV and 397 mV for WS_2-NFs and WS_2-flakes, respectively. This result revealed that using a WS_2-flower catalyst would require lower energy to generate hydrogen by water electrolysis. Furthermore, the Tafel slope of the WS_2-NFs is 92.3 mV dec^{-1} which is lower than that of the flakes WS_2 with a value of 98.1 mV dec^{-1} (Figure 3b). This demonstrates that the WS_2-NFs catalyst has faster HER reaction kinetics than the WS_2-flakes catalyst. Because the values of the Tafel slope are in the range of 40-120 mV dec^{-1}. The HER mechanism of WS_2 catalysts follows the Volmer-Heyrovsky pathway [25]. Specifically, Volmer step:

$$M + H_3O^+ + e^- \rightarrow M{-}H_{adsorption} + H_2O \qquad (2)$$

Heyrovsky step:

$$M{-}H_{adsorption} + H_3O^+ + e^- \rightarrow M + H_2 + H_2O \qquad (3)$$

M represents active sites on the surface of WS_2 materials. To confirm the reaction kinetics at the electrode and solution surfaces, impedance analysis was carried out at a specific potential of 200 mV, as shown in Figure 3c. The WS_2-NFs catalyst has a smaller Nyquist semicircle than the WS_2-flakes catalyst, indicating that the WS_2-NFs have smaller charge transfer resistance (Rct) than the WS_2-flakes catalyst. Notably, the Rct of the WS_2-NFs is 83.7 Ω, while the Rct of the WS_2-flakes is 111.7 Ω. This result confirms that the WS_2-NFs catalyst has a better charge transfer than the WS_2-flakes catalyst, revealing a faster HER kinetic. The stability of catalysts is an important factor in assessing their practical applicability. Therefore, we examined the strength of WS_2-NFs and WS_2-flakes by chronoamperometric measurement and CV. Both WS_2-NFs and WS_2-flakes catalysts showed good stability after 10 hours of continuous hydrogen generation. A slight decrease could be due to the covering of the catalytic active sites by the bubbles of hydrogen gas, as shown in Figure 3d. Moreover, the polarization curves of materials are only slightly changed compared to the initial curves, as displayed in Figure 3e and f. Notably, the overpotential at 10 mA cm^{-2} is increased only by 2 mV and 5 mV after 2000 cycles for WS_2-NFs and WS_2-flakes, respectively.

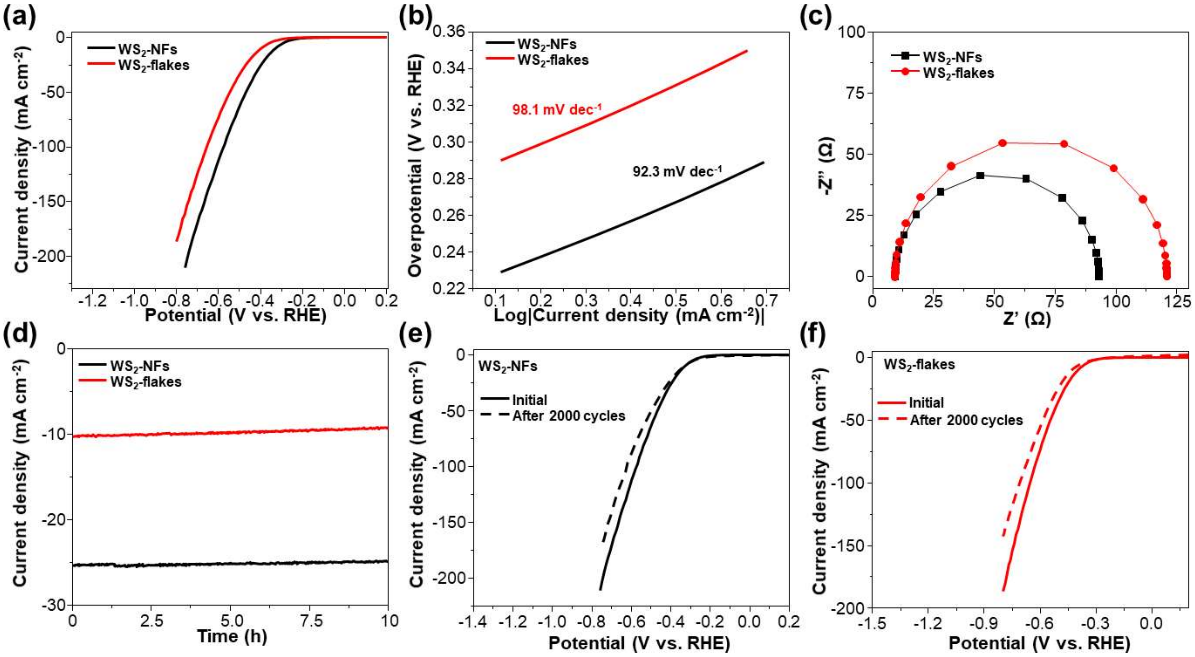

Figure 3 (a) Polarization curves of WS_2-NFs, WS_2-flakes, (b) Corresponding tafel slope of WS_2-NFs, WS_2-flakes, (c) Nyquist plots were recorded on WS_2-NFs, WS_2-flakes, (d) Chronoamperometric plots of WS_2-NFs, WS_2-flakes for 10 hours. Polarization curves were recorded initially and after 2000 CV cycles of (e) WS_2-NFs and (f) WS_2-flakes.

Electrochemical surface area (ESA) is an important parameter that can predict the electrocatalytic activity of materials. This value is usually calculated through the capacitance double layer (CDL), with the formula: ESA (cm^2) = CDL/0.035 [26]. CDL of WS_2 materials can be determined by measuring cyclic voltammetry at different scanning speeds, as exhibited in Figure 4a and b. The slope of the graph $\Delta J_{0.15}/2$ relative to the scan rate is the CDL of the material [27]. Herein, $\Delta J_{0.15}$ is the difference between anodic current density and cathodic current density at a potential of 0.15 V. The results indicated that the CDL value of WS_2-NFs in acidic media is 0.134 mF cm^{-2}, which is about two times higher than that of WS_2-flakes, as shown in Figure 4c. This result implied that the WS_2-NFs catalyst has a larger ESA than the WS_2-flakes, as shown in Figure 4d. In particular, ESA values are 3.83 cm^2 and 2.17 cm^2 for WS_2-NFs and WS_2-flakes, respectively. This result could be the main reason for better HER catalytic activity of WS_2-NFs material, as compared with WS_2-flakes.

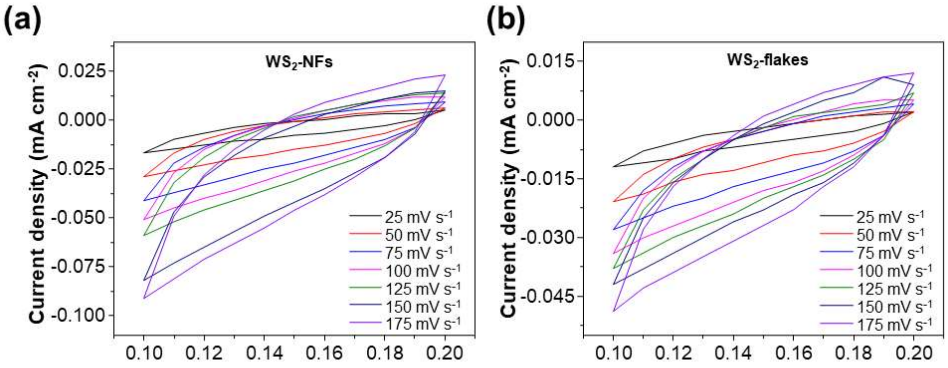

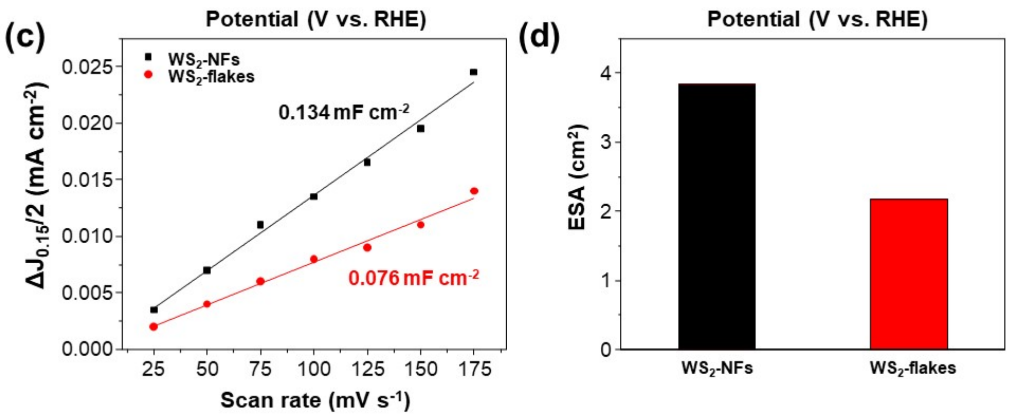

Figure 4 Cyclic voltammetry obtained in 0.5 M H_2SO_4 for (a) WS_2-NFs, (b) WS_2-flakes, (c) Extracted double-layer capacitances of WS_2-NFs, and WS_2-flakes, (d) Electrochemical surface area of WS_2-NFs, and WS_2-flakes.

The HER catalytic activities for WS_2-based electrocatalysts are provided for comparison, as shown in Table 1. The HER performance of WS_2-NFs and WS_2-flakes could be comparable with other materials such as WS_2 NF, and WS_2 NSs. This performance could be attributed to the high ESA and low Rct.

Table 1 Comparison of the HER performances of WS_2-NFs, WS_2-flakes, and against other HER electrocatalysts

Catalysts	**Overpotential (mV)**	**Tafel slope (mV dec^{-1})**	**Reference**
WS_2-NFs	325	92.3	This work
WS_2-flakes	397	98.1	This work
WS_2 NF	400	173	[19]
WS_2 NSs	160	72	[28]

4 Conclusion

In this study, different morphological structures of WS_2-NFs and WS_2-flakes were successfully fabricated for HER reaction by hydrothermal and pyrolysis methods, respectively. The results of the comparison of catalytic activity revealed that WS_2-NFs have higher HER catalytic activity than WS_2-flakes. Specifically, the WS_2-NFs require only an overpotential of 325 mV to achieve a current density of 10 mA cm^{-2}, whereas this value is 397 mV for WS_2-flakes material. Moreover, the tafel slope of WS_2-NFs is smaller than that of WS_2-flakes, which implies a faster electrochemical reaction kinetic. These results could be explained by the fact that WS_2-NFs have a larger active surface area than WS_2-flakes catalysts. Besides, both these materials displayed outstanding stability in acidic electrolytes after 10 hours of testing.

Acknowledgments

This research was funded by NTTU for Science and Technology Development under grant number 2023.01.128/HĐ-KHCN.

References

1. Li, X., Han, S., Qiao, Z., Zeng, X., Cao, D., Chen, J. (2023). Ru monolayer island doped MoS_2 catalysts for efficient hydrogen evolution reaction. *Chemical Engineering Journal* 453, 139803.

2. Li, C., Zhu, L., Wu, Z., Chen, Q., Zheng, R., Huan, J., et al. (2023). Phase Engineering of W-Doped MoS_2 by Magneto-Hydrothermal Synthesis for Hydrogen Evolution Reaction. *Small* 2303646.

3. Zhang, Y., Yang, T., Li, J., Zhang, Q., Li, B., Gao, M. (2023). Construction of Ru, O Co-Doping MoS_2 for Hydrogen Evolution Reaction Electrocatalyst and Surface-Enhanced Raman Scattering Substrate: High-Performance, Recyclable, and Durability Improvement. *Advanced Functional Materials* 33, 2210939.

4. Zou, X., Zhang, Y. (2015). Noble metal-free hydrogen evolution catalysts for water splitting. *Chemical Society Reviews* 44, 5148-80.
5. Ding, X., Yu, J., Huang, W., Chen, D., Lin, W., Xie, Z. (2023). Modulation of the interfacial charge density on Fe_2P–CoP by coupling CeO_2 for accelerating alkaline electrocatalytic hydrogen evolution reaction and overall water splitting. *Chemical Engineering Journal* 451, 138550.
6. Zhang, K., Jia, J., Yang, E., Qi, S., Tian, H., Chen, J., et al. (2023). Work-function-induced Electron Rearrangement of In-plane FeP@CoP Heterojunction Enhances All pH Range and Alkaline Seawater Hydrogen Evolution Reaction. *Nano Energy* 108601.
7. Yu, R., Du, Y.-X., Zhao, H.-F., Cao, F.-F., Lu, W.-T., Zhang, G. (2023). Crystalline/amorphous CoP/MnO_x heterostructure derived from phase separation for electrochemical catalysis of alkaline hydrogen evolution reaction. *International Journal of Hydrogen Energy* 48, 2593-604.
8. Chen, Y., Sui, T., Lyu, C., Wu, K., Wu, J., Huang, M., et al. (2023). Constructing abundant interface by decorating MoP quantum dots on CoP nanowires to induce electronic structure modulation for enhanced hydrogen evolution reaction. *Materials Horizons.*
9. Li, Z., Ge, R., Su, J., Chen, L. (2020). Recent progress in low Pt content electrocatalysts for hydrogen evolution reaction. *Advanced Materials Interfaces* 7, 2000396.
10. Yang, H., Ji, Y., Shao, Q., Zhu, W., Fang, M., Ma, M., et al. (2023). Metastable-phase platinum oxide for clarifying the Pt–O active site for the hydrogen evolution reaction. *Energy & Environmental Science* 16, 574-83.
11. Mai, H. D., Jeong, S., Bae, G. N., Tran, N. M., Youn, J. S., Park, C. M., et al. (2023). Pd Sulfidation-Induced 1T-Phase Tuning in Monolayer MoS_2 for Hydrogen Evolution Reaction. *Advanced Energy Materials* 2300183.
12. Park, J., Jeon, D., Kang, Y., Ryu, J., Lee, D. W. (2023). Nanofibrillar hydrogels outperform Pt/C for hydrogen evolution reactions under high-current conditions. *Journal of Materials Chemistry A* 11, 1658-65.
13. Shen, S., Wang, Z., Lin, Z., Song, K., Zhang, Q., Meng, F., et al. (2022). Crystalline-amorphous interfaces coupling of $CoSe_2$/CoP with optimized d-band center and boosted electrocatalytic hydrogen evolution. *Advanced Materials* 34, 2110631.
14. Zhang, L., Lei, Y., Zhou, D., Xiong, C., Jiang, Z., Li, X., et al. (2022). Interfacial engineering of 3D hollow $CoSe_2$@ultrathin $MoSe_2$ core@shell heterostructure for efficient pH-universal hydrogen evolution reaction. *Nano Research* 15, 2895-904.
15. Feng, Y., Zhang, T., Zhang, J., Fan, H., He, C., Song, J. (2020). 3D 1T-MoS_2/CoS_2 heterostructure via interface engineering for ultrafast hydrogen evolution reaction. *Small* 16, 2002850.
16. Sun, C., Zhang, J., Ma, J., Liu, P., Gao, D., Tao, K., et al. (2016). N-doped WS_2 nanosheets: a high-performance electrocatalyst for the hydrogen evolution reaction. *Journal of Materials Chemistry A* 4, 11234-8.
17. Lei, W., SHI, C.-w., YU, Z.-b., WU, H.-d., Wei, X., GENG, Z.-x., et al. (2021). Preparation of WS_2/C composite material and its electrocatalytic hydrogen evolution performance. *Journal of Fuel Chemistry and Technology* 49, 1362-70.
18. Lukowski, M. A., Daniel, A. S., English, C. R., Meng, F., Forticaux, A., Hamers, R. J., et al. (2014). Highly active hydrogen evolution catalysis from metallic WS_2 nanosheets. *Energy & Environmental Science* 7, 2608-13.
19. Hasani, A., Nguyen, T. P., Tekalgne, M., Van Le, Q., Choi, K. S., Lee, T. H., et al. (2018). The role of metal dopants in WS_2 nanoflowers in enhancing the hydrogen evolution reaction. *Applied Catalysis A: General* 567, 73-9.
20. Cao, S., Liu, T., Hussain, S., Zeng, W., Peng, X., Pan, F. (2014). Hydrothermal synthesis of variety low dimensional WS_2 nanostructures. *Materials Letters* 129, 205-08.
21. Nagaraju, C., Gopi, C. V. M., Ahn, J.-W., Kim, H.-J. (2018). Hydrothermal synthesis of MoS_2 and WS_2 nanoparticles for high-performance supercapacitor applications. *New Journal of Chemistry* 42, 12357-60.
22. Hasani, A., Van Le, Q., Tekalgne, M., Choi, M.-J., Choi, S., Lee, T. H., et al. (2019). Fabrication of a WS_2/p-Si heterostructure photocathode using direct hybrid thermolysis. *ACS Applied Materials & Interfaces* 11, 29910-6.
23. Zhang, X., Fei, H., Wu, Z., Wang, D. (2019). A facile preparation of WS_2 nanosheets as a highly effective HER catalyst. *Tungsten* 1, 101-9.

24. Pang, Q., Gao, Y., Zhao, Y., Ju, Y., Qiu, H., Wei, Y., et al. (2017). Improved lithium-ion and sodium-ion storage properties from few-layered WS_2 nanosheets embedded in a mesoporous CMK-3 matrix. *Chemistry–A European Journal* 23, 7074-80.

25. Li, Y., Wang, H., Xie, L., Liang, Y., Hong, G., Dai, H. (2011). MoS_2 nanoparticles grown on graphene: an advanced catalyst for the hydrogen evolution reaction. *Journal of the American Chemical Society* 133, 7296-9.

26. McCrory, C. C., Jung, S., Ferrer, I. M., Chatman, S. M., Peters, J. C., Jaramillo, T. F. (2015). Benchmarking hydrogen evolving reaction and oxygen evolving reaction electrocatalysts for solar water splitting devices. *Journal of the American Chemical Society* 137, 4347-57.

27. Wei, C., Sun, S., Mandler, D., Wang, X., Qiao, S. Z., Xu, Z. J. (2019). Approaches for measuring the surface areas of metal oxide electrocatalysts for determining their intrinsic electrocatalytic activity. *Chemical Society Reviews* 48, 2518-34.

28. Wu, Z., Fang, B., Bonakdarpour, A., Sun, A., Wilkinson, D. P., Wang, D. (2012). WS_2 nanosheets as a highly efficient electrocatalyst for hydrogen evolution reaction. *Applied Catalysis B: Environmental* 125, 59-66.

Nghiên cứu so sánh hoạt tính xúc tác trên các hình thái khác nhau của WS_2 cho phản ứng điện hóa tạo ra hydro

Đỗ Hữu Hà*, Đinh Đức Anh, Nguyễn Thế Duy, Nguyễn Trần Trúc Phương, Lê Đăng Mạnh
Trung tâm nghiên cứu VKTech, Viện Kĩ thuật Công nghệ cao, Trường Đại học Nguyễn Tất Thành
*dhha@ntt.edu.vn

Tóm tắt Ngày nay, sự phát triển của các chất xúc tác có độ bền cao và hiệu quả là rất quan trọng trong phản ứng tách nước tạo ra hydro (hydrogen evolution reaction – HER). Trong nghiên cứu này, ammonium metatungstate hydrate và thioacetamide được sử dụng như những tiền chất để chế tạo WS_2 hoa nano bằng phương pháp thủy nhiệt, trong khi WS_2 dạng mảnh được tạo ra từ ammonium tetrathiotungstate qua phản ứng nhiệt phân. Các cấu trúc này đã được đánh giá hoạt tính xúc tác điện hóa HER trong môi trường axit. Kết quả cho thấy WS_2 hoa nano thể hiện hoạt tính xúc tác cao hơn WS_2 dạng mảnh, với quá thế yêu cầu là 325 mV để thu được mật độ dòng 10 mA cm^{-2} và một hệ số góc Tafel 92.3 mV dec^{-1}. Hiệu suất này được cho là diện tích bề mặt hoạt tính điện hóa của WS_2 hoa nano lớn hơn so với vật liệu WS_2 dạng mảnh. Kết quả nghiên cứu này tạo tiền đề cho những nghiên cứu sâu hơn về tổng hợp vật liệu xúc tác dựa trên WS_2 đối với HER.

Từ khóa WS_2, hoa nano, hydro, xúc tác điện hóa, HER